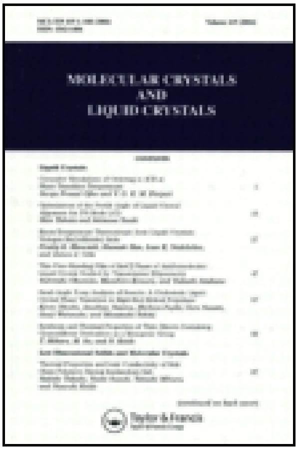

Molecular Crystals and Liquid Crystals

Raman Studies of Carbon Nanotubes and Polymer Nanotube Composites

S. Lefrant [a], J. P. Buisson [a], J. Schreiber [a], O. Chauvet [a], M. Baibarac [b] & I. Baltog [b]

[a] Laboratoire de Physique Cristalline, Institut des Matériaux Jean Rouxel, NANTES Cedex 03, France

[b] Lab. 160, BUCHAREST, National Institute of Materials Physics, Romania

Version of record first published: 18 Oct 2010

To cite this article: S. Lefrant, J. P. Buisson, J. Schreiber, O. Chauvet, M. Baibarac & I. Baltog (2004): Raman Studies of Carbon Nanotubes and Polymer Nanotube Composites, Molecular Crystals and Liquid Crystals, 415:1, 125-132

To link to this article: http://dx.doi.org/10.1080/15421400490482844

Mol. Cryst. Liq. Cryst., Vol. 415, pp. 125–132, 2004
Copyright © Taylor & Francis Inc.
ISSN: 1542-1406 print/1563-5287 online
DOI: 10.1080/15421400490482844

RAMAN STUDIES OF CARBON NANOTUBES AND POLYMER NANOTUBE COMPOSITES

S. Lefrant, J. P. Buisson, J. Schreiber, and O. Chauvet
Laboratoire de Physique Cristalline, Institut des Matériaux Jean Rouxel, BP 32229, 44322 NANTES Cedex 03, France

M. Baibarac and I. Baltog
National Institute of Materials Physics, Lab. 160, BUCHAREST, P.O. Box MG-7, R-76900 Romania

In this paper, we present Raman studies of different carbon nanotubes systems like single-walled nanotubes (SWNTs), multi-walled nanotubes (MWNTs) or composites prepared with different conjugated or non-conjugated polymers. We have focused our studies on the interactions that can take place in these systems and in general modify the characteristics of individual tubes. By introducing Van der Waals interactions between tubes, we are able to interpret experimental Raman spectra. In the case of SWNTs, we have put in evidence the so-called "bundle" effect that consists of an upshift of the frequency of the RBM of 10 to 16 cm^{-1}, depending on the size of the bundles. In MWNTs, one can calculate the low frequency Raman modes observed experimentally. We found that they originate from the radial breathing modes of isolated tubes with an upshift that depends on the number of shells constituting the tube and we were then able to calculate the intensity of such modes.

Finally, in polymer/nanotubes composites, we demonstrate that interactions take place between the two constituents in two different cases: PPV/SWNTs and PANI/SWNTs. The role of the method of preparation of composites is particularly put in evidence.

Keywords: carbon nanotubes; composites; Raman scattering; vibrational properties

This work has been carried out in the frame of an EU programme COMELCAN HPRN-CT-2000-00128.

We would like to thank E. Faulques and J. Wéry for permitting to reproduce results on PPV-SWNTs composites.

Address correspondence to S. Lefrant, Laboratoire de Physique Cristalline, Institute des Matériaux Jean Rouxel, BP 32229, Nantes, Cedex 03 44322, France. E-mail: serge.lefrant@cnrs-imn.fr

INTRODUCTION

Electronic devices based on organic materials are nowadays extensively developed for different applications such as light emitting diodes, conducting and transparent layers, electron emitters for flat panel displays, etc. [1]. These last decade, carbon nanotubes have been used in such systems, as a consequence of their electronic properties, either as pristine materials or embedded in polymers to form composites. In addition, several methods of synthesis have been developed leading to inhomogeneous tubes in terms of diameter and chirality. For potential applications, reproducible materials are needed for which characterization methods give the necessary information for a better control of the prepared compounds. In this respect, Transmission Electronic Microscopy (TEM) performed in high resolution provides a direct image of the carbon nanotubes. Resonance Raman Scattering, via the vibrations of the tubes and in particular the radial breathing modes, has also been proved to be a needed technique since it allows a determination of the diameter of the tubes [2]. On the other hand, the electronic nature of the material can be investigated by performing experiments with excitations in the red energy range [3] in resonance with transition energies of metallic tubes and excitations at either higher or lower energies revealing mostly semi-conducting tubes.

STUDIES OF VAN DER WAALS INTERACTIONS

As shown in TEM images, SWNTs are most of the time arranged in bundles, and as a consequence, vibrational frequencies can be modified, providing then non realistic information in terms of diameter distributions. For this reason, we have paid a great deal of attention to evaluate the interaction between tubes, as a starting point to characterize nanotubes, as it is the case in graphite. It is known that such interactions lead to an upshift of the vibrational frequencies. Our model [4] has been described elsewhere and we just recall here that for bundles containing an infinite number of tubes, one can predict an upshift of $\approx 16\,\mathrm{cm}^{-1}$ of the RBM frequency compared to that of a (10,10) isolated tube. This is comparable to other models found in the literature [5,6]. Such results have been proved experimentally later on fluorinated samples [7]. This chemical method of preparation permits to add fluor on nanotubes to obtain a C1.9F compound, leading also to a dispersion of the tubes. Then, a treatment with isopropanol eliminates the fluor and the nanotubes remain isolated. Raman spectra carried out either on a mica substrate, or on an Ag substrate (to perform Surface Enhanced Raman Scattering, i.e. SERS) exhibit clearly two components at $\cong 177$ and $194\,\mathrm{cm}^{-1}$. The higher frequency component decreases drastically after the fluorination/defluorination procedure. These two components have been assigned to the RBM of individual tubes and tubes in bundles, respectively. The frequency difference, $\Delta\omega \cong 17\,\text{cm}^{-1}$, is in rather good agreement with the theoretical predictions.

A careful study of Van der Waals interactions can also be performed on MWNTs [8]. In this case, interactions will take place between concentric tubes of different diameters. In fact, these investigations were conducted in order to understand the origin of the low frequency Raman bands observed below $300\,\text{cm}^{-1}$, for which no clear assignment has been given up to now [9,10].

Our calculations have been made in two steps. We first considered a n-wall tube, considering the RBM frequency ω_{oi} of each tube of radius r_i if it were isolated. We introduced new coordinates between nearest neighbour tubes with force constants derived from those found in graphite. By a diagonalisation of the dynamical matrix, we obtain new frequencies at 55, 85, 107, 122, 140 and $178\,\text{cm}^{-1}$, if we take as an example a 6-wall tube of 1.36 and 4.76 nm as internal and external diameters, respectively. This is to be compared to the frequencies 47, 55, 66, 82, 110 and $164\,\text{cm}^{-1}$, if the same tubes were isolated. As it can be seen, we do observe an upshift of the Raman bands in the right frequency range. Nevertheless, a detailed analysis of the low frequency domain, when multi-walled tubes are carefully purified, exhibit well defined features which strongly depend on the excitation wavelength. We decided to use a non-resonant theory based on a bonding polarisability model in order to determine the intensity of the Raman bands. For an isolated tube of radius r_i, the derived polarisability tensor is found to be inversely proportional to $\sqrt{r_i}$, which means that the scattering intensity is inversely proportional to r_i. In a MWNT, the total derived polarisability tensor is the sum of the tensor from each wall, multiplied by the vibration amplitude of the considered vibration mode. Considering all these parameters, we find out that in a MWNT, the inner and the outer tubes give the bigger contribution to the scattering. This puts in evidence the efficiency in these calculations of two important parameters, namely the number of walls constituting the MWNT, and the diameter of the inner tube. These two parameters can in addition be extracted experimentally from high resolution transmission electron microscopy measurements. Different simulations have been performed. First, we calculated the low frequency Raman spectrum of different tubes with the same inner diameter 1.2 nm, with 5, 10, 20 and 50 shells respectively. Second, we calculated the same Raman spectrum for MWNTs with 20 shells, but having an inner tube of diameters 0.6 nm, 1.2 nm and 2.4 nm, respectively. From experimental features, one then can deduce the most probable inner diameter which is in addition checked in TEM images and adjust both the number of shells and the relative distribution of the

MWNTs to fit experimental data. In Figure 1, we present for example simulated spectra of MWNTs in the low frequency range for two excitation wavelengths. The simulation has been made with tubes having 20 shells with inner diameters of 1.25, 1.54 and 1.7 nm, respectively.

These simulated spectra are in very good agreement with experimental Raman spectra, as it has been published elsewhere [8].

So, in conclusion of the part, the introduction of Van der Waals interactions allows us to evaluate the so-called "bundle" effect, responsible of an up-shift of $\cong$16 cm^{-1} when tubes are in bundles. This effect has been experimentally observed in isolated tubes after a fluorination/defluorinated treatment. Similar calculations in MWNTs have allowed a clear interpretation of the low frequency Raman modes that originates from radial breathing modes of individual tubes, whose frequencies are up-shifted as a consequence of the Van der Waals interactions. It must be noticed that despite the large diameters of the tube constituting the MWNTs, we do observe a large number of modes. The intensity calculations carried out in the frame of a non-resonant theory have led to the conclusion that two inverse effects are observed for the intensity: i) the smallest tubes contribute to the intensity as 1/r and ii) the smallest frequency (originating from the biggest tube) is associated with an in-phase vibration and contributes to the scattering because of cumulative effects. It remains that, even if Raman spectra can be easily simulated by introducing MWNTs with different internal diameters, the resonance behaviour has not been into

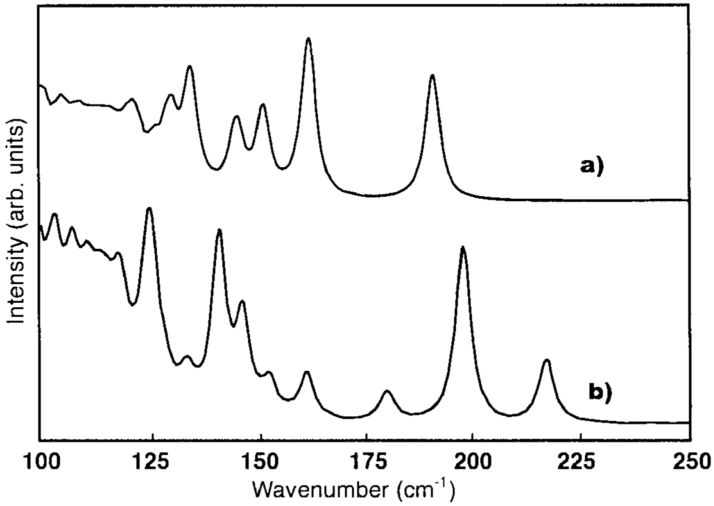

FIGURE 1 Simulation of Raman spectra of MWNTs in the low frequency range for a) $\lambda_{exc} = 514.5$ nm and b) $\lambda_{exc} = 647.1$ nm.

account and this is why different simulations are needed for Raman spectra taken at different excitation wavelengths.

STUDIES OF COMPOSITES POLYMERS/NANOTUBES

Composites are often prepared for mechanical reinforcement purpose, or to combine the properties of polymers to those of nanotubes. We already described the spectroscopic behaviour of PMMA/SWNTs composites [11] that exhibit a drastic increase of conductivity at a mass concentration of nanotubes smaller that 1%, i.e. at a very low percolation threshold. The interest is then to make a transparent and rather good conducting film that can be used as a transport layer in electronic devices. We have also shown from Raman scattering spectra an indirect confirmation of the bundle effect, since a upshift of the radial breathing mode frequencies has been demonstrated to be due to an hydrostatic pressure effect on the bundle, then hardening the force constants introduced between the tubes [12].

In this part, we will focus on composites prepared with conjugated polymers and nanotubes. Such materials have already been studied such as MEH-PPV/SWNTs [13], taking advantage of the solubility of MEH-PPV for the preparation. Here we will describe the results obtained in standard PPV/SWNTs, and also PANI/SWNTs and will show clearly that the method of preparation has a great influence of the properties of the composite material.

a) PPV-SWNTs Composites

Since standard PPV is not soluble in usual solvents, we chose a different method of preparation i.e., we mixed SWNTs at different weight concentrations in the soluble sulfonium polyelectrolyte precursor of PPV. Samples were subsequently heated under vacuum at 300° to convert the precursor polymer into PPV. We have the systematically studied composites at different SWNTs masses using optical techniques, such as U.V-visible absorption, photoluminescence and Raman scattering [14].

Figure 2 presents for example the photoluminescence spectra at RT of composites compared to that of PPV, after excitation at 2.81 eV.

Spectra are mainly composed of peaks at 2.23 eV (550 nm), a vibronic replica at 2.12 eV (575 nm) and a small component at 2.43 eV that increases gradually as a function of x. When $x = 64\%$, a new band is even observed at 2.57 eV (482 nm), which is attributed to a very short (three rings) oligomer of PPV. Notice that calculations (reported in Ref. 14) have been able to reproduce these photoluminescence (PL) spectra by introducing distributions of chain lengths and in particular short segments in the short chain distribution.

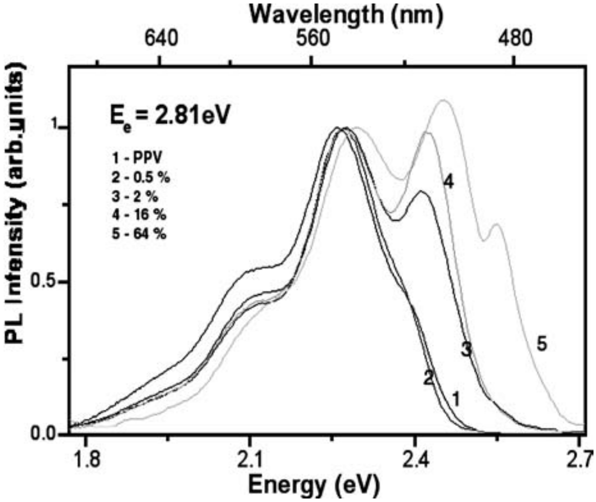

FIGURE 2 Photoluminescence spectra at RT and $\lambda_{\text{exc}} = 2.81$ eV of: 1) standard PPV; 2, 3, 4 and 5) composites PPV/SWNTs for mass concentration of 0.5%, 2%, 16% and 64% respectively. Bands are normalized to the peak of 2.23 eV.

Another efficient technique to study the chain distribution is resonant Raman scattering. As a matter of fact, the main vibrations are observed at ≅1171, 1330, 1551, 1593 and 1627 cm^{-1}. The intensities of these vibrational modes strongly depend on the chain distribution, as well as on the excitation wavelengths. In the case of composites PPV/SWNTs, it is shown that the intensity ratios I_{1551}/I_{1627} and $I/_{1171}/I_{1592}$ strongly decreases as x increases as an indication that conjugated segments are shorter when the nanotube concentration increases. Detailed results will be published elsewhere [15].

These studies put in evidence interaction between SWNTs and the precursor polymer which prevents its total conversion into PPV, with a severe limitation of the $C = C$ formation along the polymer backbone leading to short conjugated segments. This result may lead to important technological applications since it may be possible to monitor the blue emission of the samples by a proper choice of the nanotube concentration in the PPV/SWNTs composite.

b) PANI/SWNTs Composites

Composites made of polyaniline and SWNTs can be prepared by two different methods: one is by adding SWNTs in the polymer solution and the other is to perform a chemical polymerization of aniline in the presence

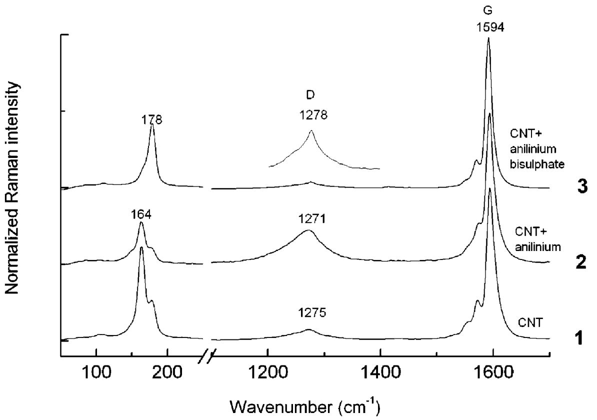

FIGURE 3 Evidence by SERS spectroscopy of the reaction of carbon nanotubes with aniline and anilinium bisulphate. Curve 1 is the SERS spectrum of SWNTs.

of SWNTs. Then two methods of preparation have led to composites with different properties, as a consequence of an irreversible chemical transformation of SWNTs in the polymerization medium [16].

Aniline reacts with carbon nanotubes to form in a first step charge transfer complexes, followed by its addition to the double bonds of the nanotubes [16]. This type of reaction is evidenced by Surface Enhanced Scattering (SERS) experiments performed with $\lambda_{\text{exc}} = 1064\,\text{nm}$, as shown in Figure 3. Compared to the SERS spectrum of SWNTs (curve 1), we observe (curve 2) that:

i) The radial breathing modes of SWNTs decreases in relative intensity, as a consequence of their transformation.
ii) The intensity ration I_{1275}/I_{1590} increases, as an indication of the creation of defects in larger concentration on nanotubes. Other studies show even bigger interaction effects with anilinium bisulphate as presented in Figure 3 (curve 3). It must be noticed in this latter case that bundling can in addition be observed by a relative disappearance of the RBM vibration at $164\,\text{cm}^{-1}$ associated with isolated nanotubes.

CONCLUSION

In this paper, we have shown the importance of Van der Waals interactions that take place in SWNTs when they are in bundles. We have theoretically determined the strength of such interactions in particular by the up-shift of the RBM frequency of $\approx 17\,\text{cm}^{-1}$ and we have demonstrated experimentally this so-called "bundle" effect. The same interaction permits also to interpret the low frequency Raman modes in MWNTs which originate from those of individual tubes. In addition, we were able to simulate Raman spectra in the low frequency range, even if resonance effects cannot be taken into account.

In composites prepared with conjugated polymers and SWNTs, namely PPV and PANI, we put in evidence interactions which modify the properties of the materials. In PPV, the photoluminescence properties are strongly affected due to the presence of nanotubes, limiting the conversion of the precursor polymer into PPV. In PANI-SWNTs composites, it is observed that aniline interacts with the nanotubes with the formation of defects and bonding on the nanotubes. These processes are of primary importance in the scope of the functionalization of the nanotubes.

REFERENCES

[1] Saito, R., Dresselhaus, G., & Dresselhaus, M. (Eds.), (1998). See for instance "*Physical properties of carbon nanotubes*", Imperial College Press: London.

[2] Rao, A. M., Richter, E., Bandow, S., Chase, B., Ecklund, P. C., Williams, K. A., Fang, S., Subbbaswamy, K. R., Menon, M., Thess, A., Smalley, R. E., Dresselhaus, G., & Dresselhaus, M. S. (1987). *Science*, *275*, 187.

[3] Brown, S. D. M., Corio, P., Marucci, A., Dresselhaus, M. S., Pimenta, M. A., & Kneipp, K. (2000). *Phys. Rev.*, *61*, R5137.

[4] Lefrant, S., Buisson, J. P., Chauvet, O., & Benoit, J. M., Baibarac, M., Baltog, I., & Bernier, P. (2001) *Proceedings of the MRS Fall Meeting*, *706*, z7.2.

[5] Henrard, L., *et al.*, (1999). *Phys. Rev.*, *B 60*, R8514.

[6] Kahn *et al.*, (1999). *Phys. Rev.*, *B 60*, 6535.

[7] Marcoux, P., Schreiber, J., Batail, P., Lefrant, S., Renouard, J., Jacob, G., Albertini, D., & Mevellec, J. Y. (2002). *J. of Royal Soc. Chem, PCCP*, *4*, 2278.

[8] Benoit, J. M., Buisson, J. P., Chauvet, O., Godon, C., & Lefrant, S. (2002). *Phys. Rev.*, *B 66*, 073417.

[9] Jantoljak, H., Salvetat, J. P., Forro, L., & Thomsen, C. (1998). *Appl. Phys. A: Mater. Sci. Process*, *67*, 113.

[10] Kataura, H., Achiba, Y., Zhao, X., & Ando, Y. (2000). In: *Amorphous and Nanostructured carbon*, Robertson, J., *et al.*, (Eds.), *MRS Symp. Proc.*, *593*, 113.

[11] Stephan, C., Nguyen, T. P., Lahr, B., Blau, W., Lefrant, S., & Chauvet, O. (2002). *J. Mat. Res.*, *17*(2), 396.

[12] Benoit, J. M., Corraze, B., Lefrant, S., Bernier, P., & Chauvet, O. (2002). *MRS 2001, Proceedings*, *706*, z3.28.

[13] Curran, S., Ajayan, P. M., Blau, W. J., Caroll, D. L., Coleman, J. N., Dalton, A. B., Davey, A. P., Drury, A., McCarthy, B., Maier, S., & Stevens, A. (1998). *Adv. Mater.*, *10*, 1091.

[14] Wery, J., Aarab, H., Lefrant, S., Faulquesz, E., Mulazzi, E., & Perego, R. (2003). *Phys. Rev.*, *B 67*, 115202.

[15] Mulazzi, E., Perego, R., Aarab, H., Lefrant, S., Faulques, E., & Wéry, J. (2003). submitted.